

# A Realistic Radiative Fermion Mass Hierarchy in Non-supersymmetric $SO(10)$

S.M. Barr and Almas Khan

Bartol Research Institute  
University of Delaware  
Newark, Delaware 19716  
(Dated: October 29, 2018)

A non-supersymmetric grand unified theory can exhibit a “radiative fermion mass hierarchy”, in which the heavier quarks and leptons get mass at tree level and the lighter ones get mass from loop diagrams. Recently the first predictive model of this type was proposed. Here it is analyzed numerically and it is shown to give an excellent fit to the quark and lepton masses and mixings, including the CP phase violating phase  $\delta_{CKM}$ . A relation between the neutrino angle  $\theta_{13}$  and the atmospheric neutrino angle is obtained.

## I. INTRODUCTION

The masses of the known quarks and leptons exhibit a large hierarchy. This has suggested to many theorists [1] that the light fermion mass hierarchy could be “radiative”, i.e. that the lightest fermions get mass from loop diagrams, while the heaviest get mass at tree level. In the early 1980’s several papers showed that such an idea can be implemented naturally in the context of non-supersymmetric grand unified theories (GUTs) [2]. In models of this type, the radiative masses come from loop diagrams containing virtual GUT-scale particles. That is why such models must be non-supersymmetric: otherwise, the loops would be suppressed by  $O(M_{SUSY}^2/M_{GUT}^2)$  due to the non-renormalization theorems of supersymmetry.

In a recent paper [3] a very simple non-supersymmetric  $SO(10)$  model with a radiative hierarchy was proposed. One thing that allows this model to be so simple is precisely that its hierarchy is radiative. The point is that terms have to exist in the lagrangian corresponding to the larger elements of the quark and lepton mass matrices, but not to the smallest elements, since they arise automatically from loops. The simplification can be seen by comparing the model of [3] to the supersymmetric  $SO(10)$  model on which it was based, which had a non-radiative hierarchy [4]. That earlier model had a somewhat larger particle content and more Yukawa terms.

Models with radiative hierarchies are also simpler in another way: in them it is not necessary to introduce *ad hoc* very small dimensionless parameters to account for the fermion mass hierarchies, since they are automatically accounted for by the loop factors  $1/16\pi^2$ . Despite radiative hierarchy models being able to have a simpler structure, one might think they would be less predictive, since loop diagrams tend to depend on many parameters. However, the model proposed in [3] shows that this need not be the case. In that paper it was shown that the model gives a qualitatively realistic pattern of quark and lepton masses and mixings with only 9 parameters.

While the non-supersymmetric model proposed in [3] is economical and qualitatively realistic, the analysis in that paper was not sufficient to establish that it is realistic quantitatively. In particular, several issues were not addressed. First, it was not specified what the sequence and scales of breaking were of  $SO(10)$  down to the Standard Model group  $G_{SM}$  (which must, of course be consistent with proton decay bounds and unification of gauge couplings). Unless that is done, the renormalization-group running of the quark and lepton masses needed for a global fit of parameters cannot be performed. Second, the forms of the mass matrices given [3] were derived under the assumption that certain  $SU(5)$ -breaking effects could be ignored. However, as will be seen, this assumption is not necessarily consistent with the pattern of  $SO(10)$  breaking that needs to be assumed in order to satisfy the constraints of gauge coupling unification and proton decay.  $SU(5)$ -breaking effects will turn out to modify significantly the forms of the quark and lepton mass matrices given in [3]. Third, the  $m_b/m_\tau$  ratio is problematic in the version of the model discussed in [3]. In that model, because certain  $SU(5)$ -breaking effects were treated as negligible, the classic prediction  $m_b^0 \cong m_\tau^0$  was obtained. (A superscript ‘0’ indicates throughout this paper quantities evaluated at the GUT scale.) This is well-known to give a fairly good fit in supersymmetric models for certain values of  $\tan \beta$  [5]; but in non-supersymmetric models it results in a prediction of  $m_b/m_\tau$  at low energies that is typically too large by at least 30% [6]. Fourth, the ratio  $m_s/m_b$  is predicted in the version of the model given in to have the Georgi-Jarlskog value  $\frac{1}{3}m_\mu/m_\tau$  at the GUT scale [7]. However, lattice calculations [8] have suggested that  $m_s$  is significantly smaller than previous estimates of it, and the best fit value is now somewhat smaller than the Georgi-Jarlskog prediction.

In this paper, we address all these issues. The paper is organized as follows. In section 2, the  $SO(10)$  model of [3] is reviewed, and it is explained how both the tree-level and radiative contributions to the mass matrices arise, and why the resulting forms give a good qualitative description of the pattern of quark and lepton masses and mixings. In section 3, a breaking of  $SO(10)$  down to the Standard Model consistent with gauge coupling unification and proton decay bounds is specified. In section 4, the effect of this pattern of symmetry breaking on the quark and lepton mass

matrices is discussed and it is shown that forms somewhat different from those given in [3] result. In section 5, the results of a global numerical fit to the quark and lepton masses and mixings is given. An excellent fit is found to the quark and lepton masses and mixings, including the CP phase  $\delta_{CKM}$ . A relation between the neutrino angle  $\theta_{13}$  and the atmospheric neutrino angle is obtained.

## II. THE MODEL

The model proposed in [3], whose predictions we analyze in detail in this paper, is a non-supersymmetric with unified group  $SO(10)$ . In it the tree-level mass matrices of quarks and charged leptons are generated by only three effective Yukawa operators

$$\begin{aligned} O_1 &= \mathbf{16}_3 \mathbf{16}_3 \mathbf{10}_H \\ O_2 &= \mathbf{16}_2 \mathbf{16}_3 \mathbf{10}_H \mathbf{45}_H / M_{GUT} \\ O_3 &= (c_i \mathbf{16}_i \mathbf{16}_{iH}) (\mathbf{16}_3 \mathbf{16}'_H) / M_{GUT} \quad , i = 1, 2 \end{aligned} \quad (1)$$

In  $O_3$ , the factors in parentheses are contracted into  $\mathbf{10}$ 's of  $SO(10)$ . The loop-level elements in the mass matrices arise very simply from the tree-level elements, as will be seen later. The three operators given in Eq. (1) do the following things:  $O_1$  gives the 33 elements of the mass matrices, i.e. the masses of the third family.  $O_2$  and  $O_3$  generate the masses of the second family and its mixing with the third family (i.e.  $V_{cb}$  and  $\theta_{atm}$ ), and also  $\theta_{sol}$ . The masses of the first family and its mixings come from loops.

The operators in Eq. (1) come from integrating out some ‘‘extra’’ vectorlike fermion multiplets, consisting of an  $SO(10)$  vector and a spinor-antispinor pair. Thus the complete fermionic content of the model comprises the following (left-handed) multiplets:  $\mathbf{16}_{i=1,2,3} + (\mathbf{16} + \overline{\mathbf{16}} + \mathbf{10})$ . The Dirac mass matrices of the up-type quarks, down-type quarks, charged leptons, and neutrinos (denoted by  $M_U$ ,  $M_D$ ,  $M_L$ , and  $M_N$ , respectively) arise from the following set of Yukawa terms in the lagrangian:

$$\begin{aligned} \mathcal{L}_{Yuk} &= M_{16} (\overline{\mathbf{16}} \mathbf{16}) + M_{10} (\mathbf{10} \mathbf{10}) \\ &+ a (\overline{\mathbf{16}} \mathbf{16}_3) \mathbf{45}_H + \sum_{i=1,2} c_i (\mathbf{10} \mathbf{16}_i) \mathbf{16}_{iH} \\ &+ h_{33} (\mathbf{16}_3 \mathbf{16}_3) \mathbf{10}_H + h_2 (\mathbf{16} \mathbf{16}_2) \mathbf{10}_H + h_3 (\mathbf{10} \mathbf{16}_3) \mathbf{16}'_H \\ &+ h (\mathbf{16} \mathbf{16}) \mathbf{10}'_H. \end{aligned} \quad (2)$$

It is shown in [3] that this form of the Yukawa interactions is the most general allowed by a certain simple  $U(1)$  flavor symmetry, which will be denoted by  $U(1)_F$ . The terms on the first line of Eq. (2) are the  $O(M_{GUT})$  masses of the extra fermion multiplets; the terms on the second line contribute  $O(M_{GUT})$  masses that mix those extra fermions with the three chiral families  $\mathbf{16}_i$ ; the terms on the third line generate the weak-scale  $SU(2)_L \times U(1)_Y$ -breaking masses; and the last term is needed to give radiative masses to the first family. Higgs multiplets are denoted by the subscript  $H$ . The Higgs fields  $\mathbf{16}_{iH}$  obtain vacuum expectation values (VEV) in the  $\mathbf{1}(\mathbf{16})$  direction. (The expression  $\mathbf{p}(\mathbf{q})$  stands for a  $\mathbf{p}$  multiplet of  $SU(5)$  contained in a  $\mathbf{q}$  multiplet of  $SO(10)$ .) The adjoint Higgs field  $\mathbf{45}_H$  is assumed to obtain a VEV that is proportional to the  $SO(10)$  generator  $B - L$  (i.e. baryon number minus lepton number).

The electroweak gauge symmetry  $SU(2)_L \otimes U(1)_Y$  is spontaneously broken by the Higgs multiplets denoted  $\mathbf{10}_H$ ,  $\mathbf{10}'_H$ , and  $\mathbf{16}'_H$  in Eq. (1), and, more specifically, by the neutral components of the  $Y/2 = -1/2$  doublets contained in  $\overline{\mathbf{5}}(\mathbf{10}_H)$ ,  $\overline{\mathbf{5}}(\mathbf{10}'_H)$ , and  $\overline{\mathbf{5}}(\mathbf{16}'_H)$ , and the neutral components of the  $Y/2 = +1/2$  doublets contained in  $\mathbf{5}(\mathbf{10}_H)$  and  $\mathbf{5}(\mathbf{10}'_H)$ . Of course, in the low-energy effective theory, which is just the Standard Model, there is only one Higgs doublet, which is some linear combination of these doublets (and their hermitian conjugates).

According to [3], the mass matrices that result from the terms in Eq. (2) have the form

$$\begin{aligned} M_U &= \begin{pmatrix} 0 & 0 & 0 \\ 0 & 0 & \frac{\epsilon}{3} \\ 0 & -\frac{\epsilon}{3} & 1 \end{pmatrix} m_U, & M_D &= \begin{pmatrix} 0 & 0 & \delta_{g1} \\ 0 & \delta_H & \frac{\epsilon}{3} + \delta_{g2} \\ C_1 & C_2 - \frac{\epsilon}{3} & 1 \end{pmatrix} m_D, \\ M_N &= \begin{pmatrix} 0 & 0 & 0 \\ 0 & 0 & -\epsilon \\ 0 & \epsilon & 1 \end{pmatrix} m_U, & M_L &= \begin{pmatrix} 0 & 0 & C_1 \\ 0 & \delta_H & C_2 - \epsilon \\ \delta_{g1} & \epsilon + \delta_{g2} & 1 \end{pmatrix} m_D, \end{aligned} \quad (3)$$

where  $m_U \equiv h_{33}\langle\mathbf{5}(\mathbf{10}_H)\rangle$  and  $m_D \equiv h_{33}\langle\bar{\mathbf{5}}(\mathbf{10}_H)\rangle$ . (It will be seen in section 4 that GUT-symmetry-breaking effects modify these forms somewhat.) The convention here is that the mass matrices are multiplied from the left by the left-handed fermions and from the right by the right-handed fermions.

The 33 elements of the mass matrices in Eq. (3) come simply from the term  $h_{33}(\mathbf{16}_3 \mathbf{16}_3)\mathbf{10}_H$ , as is usually the case in  $SO(10)$  models [9]. (This is just the operator  $O_1$  in Eq. (1).)

The contributions to the 23 and 32 elements denoted by  $\epsilon$  come from integrating out the family-antifamily pair  $\bar{\mathbf{16}} + \mathbf{16}$ . The antifamily  $\bar{\mathbf{16}}$  appears in two mass terms from Eq. (2), which can be combined as follows:  $\bar{\mathbf{16}}(M_{16}\mathbf{16} + a\langle\mathbf{45}_H\rangle\mathbf{16}_3)$ . These terms have the effect of mixing the  $\mathbf{16}$  with the  $\mathbf{16}_3$ . One linear combination of  $\mathbf{16}$  and  $\mathbf{16}_3$  obtains an  $O(M_{GUT})$  mass, while the orthogonal combination (denoted by the index  $3'$ ) remains light. (From now on, primed indices will be used to denote the light families that remain after the superheavy fermions have been integrated out.) Thus, the  $\mathbf{16}$  with no index has some of the third light family mixed in with it; and the amount of this mixing is proportional to the VEV  $\langle\mathbf{45}_H\rangle$ . As a result, the term  $h_2(\mathbf{16} \mathbf{16}_2)\mathbf{10}_H$  from Eq. (2) leads to an effective operator of the form  $(\mathbf{16}_{3'}\mathbf{16}_{2'})\mathbf{10}_H\mathbf{45}_H/M_{GUT}$ , which is just the operator  $O_2$  of Eq. (1), which in turn produces the contributions denoted in Eq. (3) by  $\epsilon$ . Since  $\langle\mathbf{45}_H\rangle \propto B - L$ , the  $\epsilon$  contributions are 1/3 times as large for the quarks as for the leptons.

The elements denoted by  $C_1$  and  $C_2$  arise in a similar fashion by integrating out the  $SO(10)$ -vector multiplet of quarks and leptons,  $\mathbf{10}$ . This multiplet contains a  $\bar{\mathbf{5}} + \mathbf{5}$  of  $SU(5)$ . The  $\mathbf{5}(\mathbf{10})$  appears in several mass terms from Eq. (2), which can be combined as  $\mathbf{5}(\mathbf{10})[M_{10}\bar{\mathbf{5}}(\mathbf{10}) + \sum_{i=1,2} c_i\langle\mathbf{1}(\mathbf{16}_{iH})\rangle\bar{\mathbf{5}}(\mathbf{16}_i)]$ . These terms have the effect of mixing the  $\bar{\mathbf{5}}(\mathbf{10})$  with the  $\bar{\mathbf{5}}(\mathbf{16}_1)$  and  $\bar{\mathbf{5}}(\mathbf{16}_2)$ . One linear combination of these  $\bar{\mathbf{5}}$ 's obtains an  $O(M_{GUT})$  mass, while the two orthogonal linear combinations are in the light families and denoted  $\bar{\mathbf{5}}_{1'}$  and  $\bar{\mathbf{5}}_{2'}$ . Consequently, the  $\bar{\mathbf{5}}(\mathbf{10})$  has mixed in with it some of  $\bar{\mathbf{5}}_{1'}$  and  $\bar{\mathbf{5}}_{2'}$ . That means that the term  $h_3(\mathbf{10} \mathbf{16}_3)\mathbf{16}'_H$  in Eq. (2) leads to effective mass terms of the form  $(C_1\bar{\mathbf{5}}_{1'} + C_2\bar{\mathbf{5}}_{2'})\mathbf{10}_3 m_D$ . This is just the operator  $O_3$  of Eq. (1) and gives the terms denoted by the  $C_i$  in Eq. (3). These contributions appear only in  $M_L$  and  $M_D$ , because  $\bar{\mathbf{5}}$ 's of  $SU(5)$  contain only charged leptons and down-type quarks. In both [4] and [3] the  $M_{10}$  was assumed to be an explicit (and therefore  $SU(5)$ -invariant) mass, and therefore the same  $C_i$  appear in both  $M_L$  and  $M_D$ .

At this point it should be noted that the expressions for the quark and lepton mass matrices given in Eq. (3) are approximate. The exact expressions involve factors, such as  $1/\sqrt{1 + (a\langle\mathbf{45}_H\rangle/M_{16})^2}$  and  $1/\sqrt{1 + (\sum_i c_i\langle\mathbf{16}_{iH}\rangle/M_{10})^2}$ , which are essentially just the cosines of angles describing the mixing between the extra fermions  $\mathbf{16} + \bar{\mathbf{16}} + \mathbf{10}$  and the three chiral families  $\mathbf{16}_i$ . If these mixing angles are small, their cosines are very close to one, and the mass matrices become insensitive to their values. This is an assumption that we make here (as in [3]), as it reduces the number of parameters. However, there is no *a priori* reason to assume that these angles are extremely small. (Indeed, if they vanished, so would  $\epsilon$ .) If one of these angles were of order 0.25 radians, say, it would give 3% corrections to some of the elements of the mass matrices.

The elements denoted by  $\delta_{gi}$  and  $\delta_H$  in Eq. (3) are necessary to make the mass matrices  $M_L$  and  $M_D$  be of rank 3 rather than rank 2, and so generate masses and mixings for the first family. As will be seen, in order to fit the first family masses and mixings these  $\delta$  are must be of order  $10^{-2}$ , whereas the other parameters appearing inside in the mass matrices in Eq. (3) turn out to be of order 1 (or, in the case of  $\epsilon$ , about 0.19). In [4], additional vectorlike quark and lepton fields besides those in Eq. (2) had to be introduced in order to generate these small  $\delta$ 's. In [3], however, it was noted that that the terms in Eq. (2) are enough to generate the  $\delta$  terms automatically by one-loop diagrams and also to explain why they are of order  $10^{-2}$ .

The  $\delta_{gi}$  terms are given by the one-gauge-boson-loop diagram shown in Fig. 1(a). The gauge boson in this diagram is in a  $\mathbf{10}$  of  $SU(5)$  (of course, it is in the adjoint  $\mathbf{45}$  of  $SO(10)$ ), so that it turns  $\mathbf{10}$ 's of  $SU(5)$  into  $\bar{\mathbf{5}}$ 's and *vice versa*. That means that the small  $\delta_{gi}$  elements that couple  $\mathbf{10}_i$  to  $\bar{\mathbf{5}}_3$  (namely  $(M_D)_{i3}$  and  $(M_L)_{3i}$ ) come from the large  $C_i$  elements that couple  $\bar{\mathbf{5}}_i$  to  $\mathbf{10}_3$  (namely  $(M_L)_{i3}$  and  $(M_D)_{3i}$ ) So  $\delta_{gi} \propto C_i$ . These diagrams were evaluated in [3] neglecting certain  $SU(5)$ -breaking effects, giving the result that the same  $\delta_{gi}$  appear in  $M_L$  and  $M_D$ , as given in Eq. (3).

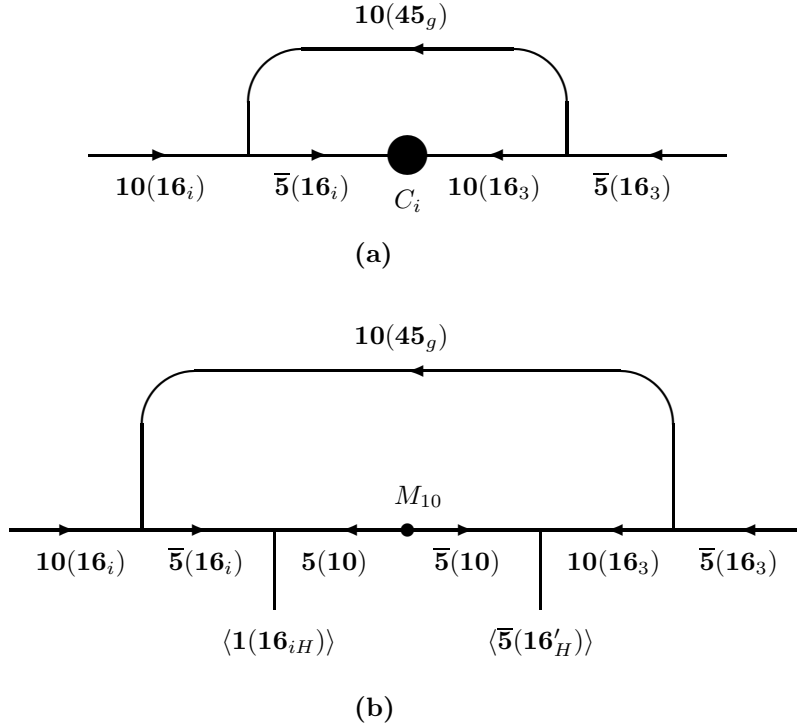


**Figure 1.** The diagram in (a) shows how a tree-level mass for  $\mathbf{10}_3\bar{\mathbf{5}}_i$  (shown as a blob in the center) leads to a one-loop mass for  $\mathbf{10}_i\bar{\mathbf{5}}_3$ : i.e. the  $\delta_{gi}$  elements arise radiatively from the  $C_i$  elements. The  $\mathbf{10}(45_g)$  in the loop is a superheavy gauge boson. The diagram in (b) is more detailed and shows why the loop is finite.

The diagram in Fig 1(a) superficially looks divergent. However, the accidental symmetry  $U(1)_F$  of the terms in Eq. (1) makes  $(M_D)_{13}$  and  $(M_L)_{31}$  vanish at tree level and guarantees that the loop is finite, as an exact calculation indeed shows. The finiteness of this diagram is more obvious if we write it in the form shown in Fig. 1(b). The calculation of these loops will be discussed in section 4.

The 22 elements of  $M_L$  and  $M_D$  (denoted  $\delta_H$ ) arise from the one-Higgs-boson-loop diagram shown in Fig. 2. Whereas the one-gauge-boson-loop shown in Fig. 1 *must* exist if the tree-level masses in Eq. (3) exist, the diagram in Fig. 2 only exists if certain couplings not needed for the tree-level masses are present: namely, the last term in Eq. (2) ( $h(\mathbf{16}\ \mathbf{16})\ \mathbf{10}'_H$ ) and a Higgs-mass term of the form  $\mathbf{10}_H\mathbf{10}_H$ . A diagram related by  $SO(10)$  to the one in Fig. 2 gives a 22 element for the up-quark mass matrix  $M_U$ . However, if one supposes the contributions to  $(M_U)_{22}$  and  $(M_D)_{22}$  from these diagrams to be roughly comparable, then  $(M_U)_{22}/(M_U)_{33}$  would be of order  $10^{-4}$  and thus at most a few percent correction to  $m_c$ .

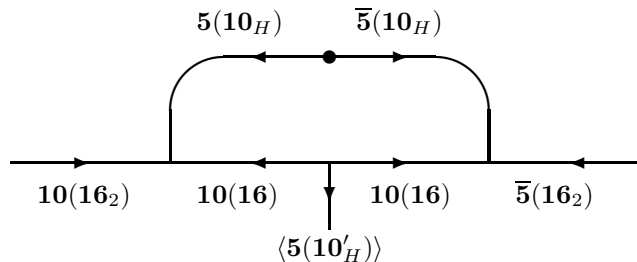


**Figure 2.** A diagram showing how the 22 elements of the mass matrices can arise radiatively through Higgs-boson loops.

Before getting into a more detailed discussion of the model, it is useful to explain how the structure of the matrices given in Eq. (3) explains qualitatively many of the features of the observed pattern of masses and mixings of the quarks and leptons.

First, neglecting the  $\delta$  parameters (which are of order  $10^{-2}$  because they come from one-loop diagrams) and the parameter  $\epsilon$  (which, though a tree-level effect, is somewhat smaller than 1), one has that all the mass matrices in Eq. (3) are of rank 1. In this approximation,  $m_b^0 \cong m_\tau^0 \cong \sqrt{1 + |C_1|^2 + |C_2|^2}$ , where the superscript ‘0’ denotes quantities evaluated at the GUT scale. The relation  $m_b^0 \cong m_\tau^0$  is known to fit fairly well in supersymmetric grand unified models with certain values of  $\tan\beta$ . It works less well in non-supersymmetric grand unified models; however, this relation will be substantially modified when realistic symmetry breaking is taken into account in section 4.

The large (i.e.  $O(1)$ ) off-diagonal elements  $C_i$  produce large mixing angles in the left-handed lepton sector and the right-handed quark sector. This is because they result from mixings of  $\bar{\mathbf{5}}$ ’s of  $SU(5)$ , which contain, of course, left-handed charged leptons and right-handed down-type quarks. Consequently, these elements produce large MNS neutrino mixing angles, but they do not produce large CKM mixing, since CKM mixing is of the left-handed not right-handed quarks. This is one of the basic ideas of so-called “lopsided” models [10].

Moreover, the present model is “doubly lopsided” in the sense that both  $C_1$  and  $C_2$  are large [11]. (In singly lopsided models  $C_2$  is large but not  $C_1$ .) This doubly lopsided structure can give a very simple explanation of the “bi-large” pattern of neutrino mixing angles in the following way. Diagonalizing the charged-lepton mass matrix  $M_L$  requires  $O(1)$  rotations to eliminate the elements  $C_1$  and  $C_2$ . In particular, it requires a rotation by  $\theta_s = \tan^{-1}(C_1/C_2)$  in the 1-2 plane followed by a rotation by  $\theta_a = \tan^{-1} \sqrt{|C_1|^2 + |C_2|^2}$  in the 2-3 plane. If, as here, the neutrino mass matrix is hierarchical, then the rotations required to diagonalize the charged lepton mass matrix  $M_L$  give the dominant contributions to the MNS matrix, which is therefore approximately of the form

$$U_{MNS} = \begin{pmatrix} c_s & s_s & 0 \\ -c_a s_s & c_a c_s & s_a \\ s_a s_s & -s_a c_s & c_a \end{pmatrix}, \quad (4)$$

where  $s_a \equiv \sin\theta_a$ ,  $c_a \equiv \cos\theta_a$ ,  $s_s \equiv \sin\theta_s$ , and  $c_s \equiv \cos\theta_s$ . This is the bi-large form, with  $\theta_s$  being the solar neutrino angle and  $\theta_a$  being the atmospheric angle. When the effects of the small parameters  $\epsilon$  and the  $\delta$ ’s are taken into account, there will be small shifts in  $U_{MNS}$ , including a small non-zero  $\theta_{13}$ , which will be calculated in section 5.

If one considers the effects of  $\epsilon$ , but still neglects the  $\delta$ ’s, one sees by inspection of the mass matrices in Eq. (3) that  $m_c/m_t$  is of order  $\epsilon^2$ , whereas  $m_s/m_b$ ,  $m_\mu/m_\tau$  and  $V_{cb}$  are all of order  $\epsilon$ . This corresponds to the experimental fact that  $m_c/m_t \simeq 0.0025$ , whereas  $m_s/m_b$ ,  $m_\mu/m_\tau$ , and  $V_{cb}$  are given respectively by 0.02, 0.06, and 0.04. In fact, it is easy to show from Eq. (2) that  $V_{cb}^0 \simeq \frac{\epsilon}{3} \sin^2\theta_a$  and  $(m_s/m_b)^0 \simeq \frac{\epsilon}{3} \sin\theta_a \cos\theta_a$ , so that  $V_{cb} \sim m_s/m_b$ , in agreement with observation. One also easily sees that  $(m_s/m_b)^0 \simeq \frac{1}{3} \epsilon \frac{C}{1+C^2}$  and  $(m_\mu/m_\tau)^0 \simeq \epsilon \frac{C}{1+C^2}$ , where  $C \equiv \sqrt{|C_1|^2 + |C_2|^2}$ , so that the ratio  $(m_s/m_b)^0 / (m_\mu/m_\tau)^0$  is approximately 1/3, the Georgi-Jarlskog prediction [7].

The  $u$  quark is left massless by the matrices in Eq. (3). However, that is not a bad thing. Experimentally,  $m_u/m_t$  is of order  $10^{-5}$ , which is far smaller than the corresponding ratios  $m_d/m_b \sim 10^{-3}$  and  $m_e/m_\tau \sim 0.3 \times 10^{-3}$ . Thus, if  $m_d$  and  $m_e$  arise at one-loop level, one would expect  $m_u$  to vanish at one-loop level.

Before analyzing the structure of the quark and lepton mass matrices further, it is necessary to deal with the question of the pattern of breaking of  $SO(10)$  down to the Standard Model group  $G_{SM} = SU(3)_c \otimes SU(2)_L \otimes U(1)_Y$ .

### III. THE BREAKING OF $SO(10)$

If  $SO(10)$  broke at a single scale all the way to the Standard Model group  $G_{SM}$ , it would give the same prediction for the low energy gauge couplings as non-supersymmetric  $SU(5)$ , which are known to be unsatisfactory. Moreover, as in non-supersymmetric  $SU(5)$ , the proton lifetime would be too short. However, it is possible to get satisfactory gauge coupling unification and proton lifetime by assuming a two-stage breaking with the Pati-Salam group [12] as the intermediate symmetry:

$$SO(10) \xrightarrow{M_G} SU(4)_C \otimes SU(2)_L \otimes SU(2)_R \xrightarrow{M_{PS}} SU(3)_C \otimes SU(2)_L \otimes U(1)_Y$$

The breaking of  $SO(10)$  to the Pati-Salam group at the higher scale  $M_G$  can be done by a  $\mathbf{210}_H$ . The breaking of the Pati-Salam group at  $M_{PS}$  is done by the VEVs of the adjoint and spinor Higgs fields,  $\mathbf{45}_H$  and  $\mathbf{16}_{iH}$ , which also contribute to the superheavy quark and lepton masses through couplings that appear in Eq. (2).

In running the gauge couplings between  $M_G$  and  $M_{PS}$ , the following matter multiplets contribute to the beta functions: (1) The quark and lepton multiplets,  $\mathbf{16}_1$ ,  $\mathbf{16}_2$ ,  $\mathbf{16}_3$ ,  $\mathbf{16}$ ,  $\overline{\mathbf{16}}$ , and  $\mathbf{10}$ . Since the masses of these multiplets are produced by coupling to the adjoint and spinor Higgs fields and not the  $\mathbf{210}_H$ , their splittings are of order  $M_{PS}$  and can be ignored in running between  $M_G$  and  $M_{PS}$ . (2) The Higgs multiplets  $\mathbf{16}_{1H}$ ,  $\mathbf{16}_{2H}$ ,  $\mathbf{16}'_H$ ,  $\mathbf{10}_H$ ,  $\mathbf{10}'_H$ , and three adjoint Higgs multiplets. For the Higgs multiplets too, except for the adjoints, it is assumed that the splittings are of order  $M_{PS}$  and can be neglected in running between  $M_G$  and  $M_{PS}$ . For the adjoints, however, we assume splittings of order  $M_G$ . Under the Pati-Salam group a  $\mathbf{45}_H$  decomposes to  $(15, 1, 1)_H + (6, 2, 2)_H + (1, 3, 1)_H + (1, 1, 3)_H$ . We assume that the color-singlet pieces of the adjoints get mass of order  $M_G$  and the color-non-singlet pieces get mass of order  $M_{PS}$ . This is not unreasonable, since the renormalizable couplings of the adjoints to the  $\mathbf{210}_H$  produce splittings of order  $M_G$  between the color-singlet and color-non-singlet pieces. (One such term is  $\langle H^{[IJKL]} \rangle H^{[IJ]} H^{[KL]}$ , where the fundamental indices  $I, J, K, L$  take  $SU(2)_L \otimes SU(2)_R$  values.) Of course, the whole Higgs potential must be tuned to give the hierarchy between  $M_G$  and  $M_{PS}$ , so different patterns of splittings are possible. It is in order to get a value of  $M_G$  large enough to be consistent with proton-decay limits, that we assume there are three split adjoint Higgs multiplets. More such adjoints would push  $M_G$  higher. Below the scale  $M_{PS}$ , we assume just the Standard Model field content with one Higgs doublet.

The results of the running are shown in Fig. 3.

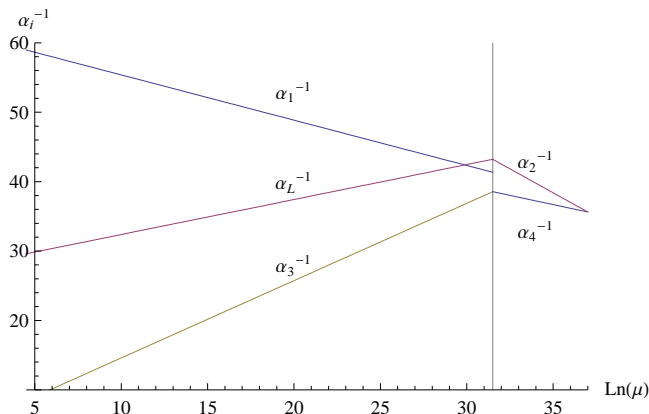


**Figure 3.** The running of the gauge couplings. The Pati-Salam scale is indicated by the vertical line.

In the running, the input values used are  $\alpha_1^{-1}(M_Z) = 58.97$ ,  $\alpha_2^{-1}(M_Z) = 29.61$ , and  $\alpha_3^{-1}(M_Z) = 8.47$  [14]. The result of the running is that  $M_{PS} = 4.79 \times 10^{13}$  GeV. At  $M_{PS}$  the Standard Model couplings have the values  $\alpha_1^{-1}(M_{PS}) = 41.35$ ,

$\alpha_2^{-1}(M_{PS}) = 43.21$ , and  $\alpha_3^{-1}(M_{PS}) = 38.55$ . The unification scale comes out to be  $M_G = 1.17 \times 10^{16}$  GeV. and  $\alpha_U^{-1}(M_G) = 35.65$ . These values are consistent with present bounds on proton decay. (In this model, the dominant contribution to proton decay comes from dimension-6 operators produced by the exchange of gauge bosons of mass  $M_G$ . The Pati-Salam gauge bosons do not give proton decay.) The values of the gauge couplings plotted in Fig. 3 are used in the running of the quark and lepton masses and mixing angles in section 5.

One consequence of the fact that  $SO(10)$  is broken down to the Pati-Salam group at a high scale is that it makes more natural the assumption being made in this model that  $\langle \mathbf{45}_H \rangle \propto B - L$ . In the original supersymmetric version of the model [4] this assumption was justified by the fact that a  $\mathbf{45}_H$  whose VEV is proportional to  $B - L$  is needed to implement to Dimopoulos-Wilczek mechanism (or “missing VEV mechanism”) [13] for doublet-triplet splitting. However, in a non-supersymmetric  $SO(10)$  model, that mechanism does not work — and, in fact, doublet-triplet splitting must be achieved through fine-tuning [15]. The justification for the assumption made in [3] that  $\langle \mathbf{45}_H \rangle \propto B - L$  is therefore less clear. However, if  $SO(10)$  breaks to the Pati-Salam group at the high scale  $M_G$  in such a way that only the  $(1, 3, 1)_H + (1, 1, 3)_H$  in the adjoints have the large mass  $M_G$ , as assumed, then the residual  $(15, 1, 1)_H$  naturally obtains a VEV in the  $B - L$  direction (and, in fact can do no other without breaking the Standard Model group at a superheavy scale).

#### IV. MODIFICATIONS TO THE MASS MATRICES

In this section the implications for the mass matrices of the breaking of  $SO(10)$  down to the Pati-Salam group will be analyzed.

In Eq. (3) the term  $M_{10}(\mathbf{10} \mathbf{10})$ , as written, involves an explicit mass. This was the assumption made in [3]. It is also possible, however, and just as simple, to suppose that this mass arises from the VEV of some Higgs fields that breaks  $SO(10)$ . For example the term may come from  $(\mathbf{10} \mathbf{10})\langle \mathbf{45}_H \rangle\langle \mathbf{45}_H \rangle/M_{PS}$  or from  $(\mathbf{10} \mathbf{10})\langle \mathbf{54}_H \rangle$ . If  $M_{10}$  reflects the breaking of  $SU(5)$  then it is a matrix that gives different values when acting on the down quarks and on the charged leptons in the  $SO(10)$   $\mathbf{10}$  of fermions. Call its value for the leptons  $M$  and for the down quarks  $M'$ . One result of this splitting is that the entries  $C_i$  are no longer the same in the mass matrices  $M_L$  and  $M_D$ . If one assumes, as before, that the quantities  $\sqrt{1 + (\sum_i c_i \langle \mathbf{16}_{iH} \rangle / M_{10})^2}$  are well approximated by 1, then one can write the  $C_i$  contributions to the mass matrices as  $C_i$  for  $M_L$  and  $fC_i$  for  $M_D$ , where  $f = M/M'$ . This  $SO(10)$ -breaking effect is, as it were, optional. However, it is quite important for fitting  $m_b^0/m_\tau^0$ , which otherwise would be predicted to be 1. The effects that will now be described are unavoidable consequences of the breaking of  $SO(10)$ .

$SO(10)$ -breaking and  $SU(5)$ -breaking effects come into the loop contributions  $\delta_{g_i}$  and  $\delta_H$  in several ways. Consider  $\delta_H$  first. If one examines the diagram in Fig. 2 closely, one finds that its contribution to  $M_D$  involves loops with scalars that can be either color triplets or color singlets, whereas its contributions to  $M_L$  involve only color-triplet scalars. When  $SO(10)$  breaks to the Pati-Salam group, the degeneracy between these two types of scalars is badly broken, which means that one cannot assume that Fig. 2 gives the same contribution to the two matrices. We therefore introduce a factor  $f_H$  into the 22 element of  $M_L$  to reflect this fact.

The case of the elements  $\delta_{g_i}$  requires a more involved discussion. First, it must be noted that the vacuum expectation values  $\langle \mathbf{1}(\mathbf{16}_{iH}) \rangle$  and  $\langle \mathbf{45}_H \rangle$  break the Pati-Salam group, and therefore must be no larger than  $M_{PS}$ . Moreover, the masses  $M_{10}$  and  $M_{16}$  cannot be too much larger than these VEVs, since otherwise the entries  $C_i$  and  $\epsilon$  would be too small. Consequently, one can assume that all the superheavy fermion masses are much lighter than the scale  $M_G$ . This has implications for the loop diagrams in Fig. 1. Some of those diagrams contain gauge bosons whose mass is of order  $M_{PS}$  and others contain gauge bosons whose mass is of order  $M_G$ . Because the fermions in those loops are much lighter than  $M_G$ , as just argued, the loops with  $O(M_G)$  gauge bosons are suppressed relative to the loops with  $O(M_{PS})$  gauge bosons by a large factor and are therefore negligible. To see what this implies, one must look in more detail at the diagrams in Fig. 1 to see how they contribute to  $M_L$  and  $M_D$ .

In Fig. 4(a), is shown the contribution to  $M_L$ . In this diagram there are three possible values of the color index  $a$ , (or, equivalently, of the pair of color indices  $bc$  on the superheavy gauge boson  $X^{bc}$ ). For any of these values, the gauge boson converts a left-handed charged lepton into a left-handed down-type quark at one vertex, and a left-handed charged anti-lepton into a left-handed down-type anti-quark at the other vertex. That shows that the gauge boson is one of those of the Pati-Salam group  $SU(4)_c$ , which make such transitions. (The Pati-Salam multiplet  $(\mathbf{4}, \mathbf{2}, \mathbf{1})$  unifies left-handed leptons and quarks, while the multiplet  $(\bar{\mathbf{4}}, \mathbf{1}, \mathbf{2})$  unifies left-handed anti-leptons and anti-quarks.) For all three values of  $a$ , therefore, the loop in Fig. 3(a) contains only gauge bosons whose mass is of order  $M_{PS}$ .

In Figs. 4(b) and 4(c) are shown the diagrams that contribute to  $M_D$ . In Fig. 4(b), the external quark has a color index of fixed value  $a$ , which determines uniquely the values of the color indices on the virtual gauge boson  $X^{bc}$ . This gauge boson is (as in Fig. 4(a)) one of those of the Pati-Salam group  $SU(4)_c$ , as can be seen from the fact that it converts left-handed down quarks into left-handed charged leptons. In Fig. 4(c) there are two choices for the color index  $c$  on the gauge boson  $X^{1c}$ , since it is only required to be different from  $a$ . This gauge boson, however, is

obviously *not* one of those of the Pati-Salam group, since it converts a left-handed quark into a left-handed anti-quark (and a left-handed lepton into a left-handed anti-lepton), which are not unified together in the multiplets of the Pati-Salam group. Thus the gauge boson in Fig. 4(c) has mass of order  $M_G \gg M_{PS}$ . The diagram in Fig. 4(c) is thus highly suppressed. From these considerations, one sees that the contribution to  $M_L$  has a factor 3 relative to the contribution to  $M_D$  because of the color degeneracy in the loop.

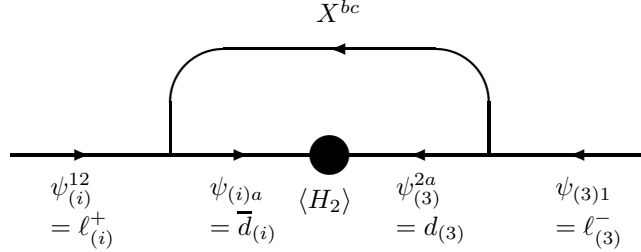


Fig. 4(a)

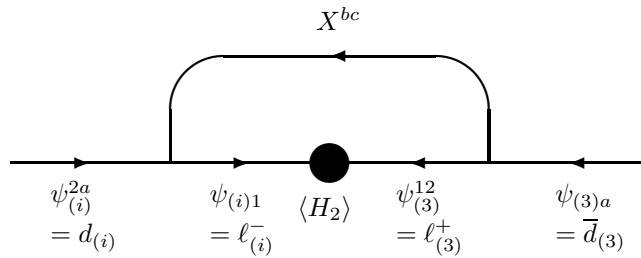


Fig. 4(b)

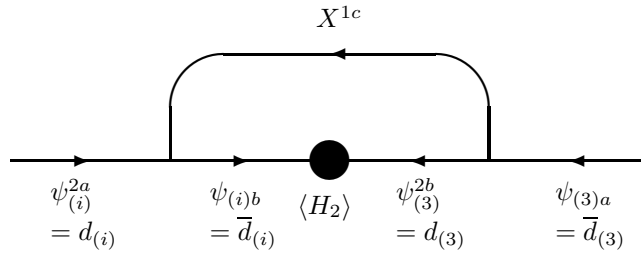


Fig. 4(c)

**Fig. 4** Gauge-boson-loop contribution to mass matrices. Subscripts in parentheses are family labels.  $a, b, c$  are  $SU(3)_c$  indices. 1, 2 are  $SU(2)_L$  indices.

The gauge-boson-loop integrals can be written in a simple form if one makes the same approximation as before, namely  $\sqrt{1 + (\sum_i c_i \langle \mathbf{16}_{iH} \rangle / M_{10})^2} \cong 1$ . In that case the gauge-boson-loop contributions to  $M_L$  and  $M_D$  are given by

$$\begin{aligned} (M_L)_{3i}^{gbl} &= 3 \left( \frac{3\alpha_U}{16\pi^2} \right) C_i \frac{\ln x}{x-1}, \\ (M_D)_{i3}^{gbl} &= \left( \frac{3\alpha_U}{16\pi^2} \right) (f C_i) \frac{\ln x'}{x'-1}. \end{aligned} \quad (5)$$

Here  $x \equiv (M_g/M)^2$  and  $x' \equiv (M_g/M')^2$ , where  $M_g$  is the mass of the colored ‘‘Pati-Salam’’ gauge bosons in Fig. 3(a) and 3(b). Recalling that  $f = M/M'$ , one can rewrite these as



$$\begin{aligned}
(M_L)_{3i}^{gb\ell} &= 3 \left( \frac{3\alpha_U}{16\pi^2} \right) C_i \left( \frac{M}{M_g} \right) F(x), \\
(M_D)_{i3}^{gb\ell} &= \left( \frac{3\alpha_U}{16\pi^2} \right) C_i \left( \frac{M}{M_g} \right) F(x'),
\end{aligned} \tag{6}$$

where  $F(x) \equiv x^{1/2} \ln x / (x - 1)$ . It happens that the function  $F(x)$  is very slowly varying for arguments of order 1. For example,  $F(1 + y) = 1 - \frac{1}{24}y^2 + \frac{1}{24}y^3 + \dots$ , and  $F(2) = F(\frac{1}{2}) = 0.98$ . Thus to a very good approximation one may write

$$\begin{aligned}
(M_L)_{3i}^{gb\ell} &= 3C_i\delta \\
(M_D)_{i3}^{gb\ell} &= C_i\delta.
\end{aligned} \tag{7}$$

The mass matrices that result are

$$\begin{aligned}
M_U &= \begin{pmatrix} 0 & 0 & 0 \\ 0 & 0 & \frac{\epsilon}{3} \\ 0 & -\frac{\epsilon}{3} & 1 \end{pmatrix} m_U, & M_D &= \begin{pmatrix} 0 & 0 & C_1\delta \\ 0 & \delta_H & \frac{\epsilon}{3} + C_2\delta \\ fC_1 & fC_2 - \frac{\epsilon}{3} & 1 \end{pmatrix} m_D, \\
M_N &= \begin{pmatrix} 0 & 0 & 0 \\ 0 & 0 & -\epsilon \\ 0 & \epsilon & 1 \end{pmatrix} m_U, & M_L &= \begin{pmatrix} 0 & 0 & C_1 \\ 0 & f_H\delta_H & C_2 - \epsilon \\ 3C_1\delta & \epsilon + 3C_2\delta & 1 \end{pmatrix} m_D,
\end{aligned} \tag{8}$$

## V. FITTING THE FERMION MASSES AND MIXINGS

The forms of the mass matrices in Eq. (8) are those given by the model at the scale  $M_{PS}$ , since that is the mass of the superheavy fields that are integrated out to give these matrices. Below  $M_{PS}$ , the model reduces to the Standard Model. One can therefore use the renormalization group equations (RGEs) of the one-Higgs-doublet Standard Model to run the measured quark and lepton masses and mixings from low scales up to  $M_{PS}$  and then fit the results using the forms in Eq. (8).

Running from  $M_Z$  to  $M_{PS}$  is done using the one-loop Standard Model RGEs given in [16]. The input values of the quark and lepton masses at  $M_Z$ , shown in Table I, are taken from [17], and were computed using updated Particle Data Group values.

$m_u$	$1.27 \pm 0.50$ MeV
$m_s/m_d$	$19.9 \pm 0.8$
$m_s$	$55 \pm 16$ MeV
$m_c$	$0.619 \pm 0.084$ GeV
$m_b$	$2.89 \pm 0.09$ GeV
$m_t$	$171.7 \pm 3$ GeV
$m_e$	$0.486\,570\,161 \pm 0.000\,000\,042$ MeV
$m_\mu$	$102.718\,135\,9 \pm 0.000\,00\,92$ MeV
$m_\tau$	$1746.24 \pm 0.20$ MeV

Table I.

The input values of the CKM angles are taken from [18]:  $s_{12} = 0.2243 \pm 0.0016$ ,  $s_{23} = 0.0413 \pm 0.0015$ , and  $s_{13} = 0.0037 \pm 0.0005$ . The leptonic angles are taken from [19]:  $\theta_{sol} = 33.9^\circ \pm 2.4^\circ$ ,  $\theta_{atm} = 45^\circ \pm 10^\circ$ . The quark and lepton masses at  $M_{PS}$  that result from the running are shown in Table II.

	mass with error bar	fractional error(%)
$m_u$	$0.571 \pm 0.24$ MeV	42
$m_s/m_d$	$18.9 \pm 0.8$	4.23
$m_s$	$25.387 \pm 8.0$ MeV	31
$m_c$	$0.278 \pm 0.042$ GeV	15
$m_b$	$1.186 \pm 0.05$ GeV	4.2
$m_t$	$86.926 \pm 4$ GeV	4.6
$m_e$	$0.488848231 \pm 0.000\ 000\ 042$ MeV	$10^{-5}$
$m_\mu$	$103.199\ 06\ 11 \pm 0.000\ 00\ 92$ MeV	$10^{-5}$
$m_\tau$	$1754.46 \pm 0.20$ MeV	$10^{-4}$

**Table II.**

The quark mixing angles at the Pati-Salam scale are,  $s_{12} = 0.2243 \pm 0.0016$ ,  $s_{23} = 0.0464 \pm 0.0015$  and  $s_{13} = 0.0041 \pm 0.0005$ .

Note that we fit  $m_d/m_s$ , which is relatively well-known from current algebra, rather than fitting  $m_d$  itself. For several quantities, namely the charged lepton masses, the mass of the  $u$  quark, and the atmospheric neutrino angle, we will add a ‘‘theoretical error bar’’ to the experimental error bar in doing the  $\chi^2$  fit. In the case of the charged leptons, we add a 1% fractional error to their masses, simply because we do not expect the forms in Eq. (8) to be more accurate than that. (We have made approximations of that order in deriving them.)

In the case of  $m_u$ , we add a theoretical error because the mass matrices we are using to do the fit include only tree-level and one-loop effects. A two-loop contribution to the 11 element of  $M_U$  would be expected to be roughly of order  $(\frac{1}{16\pi^2})^2 m_t^0 \sim 3.5$  MeV. Thus we take the prediction of the model to be that  $m_u^0 = 0 \pm 3.5$  MeV. In other words, the theoretical error for  $m_u$  is about 600% of the actual value of  $m_u$ , so it has no effect on the fitting.

In the case of the atmospheric neutrino angle, there is an inherent uncertainty in the prediction of this model, due to the Majorana mass matrix of the right-handed neutrinos  $M_R$  being unknown and not predicted by the model. Because the Dirac neutrino mass matrix  $M_N$  is (to one-loop order) given by the form in Eq. (8), which has vanishing first row and column, it follows that the light neutrino mass matrix, given by the usual type-I see-saw formula  $M_\nu = -M_N^T M_R^{-1} M_N$ , also has vanishing first row and column. Thus, the unitary matrix  $U_\nu$  required to diagonalize  $M_\nu$  is simply a rotation by some angle  $\theta_\nu$  in the 23 plane. From the form of  $M_N$ , one expects generically that  $\theta_\nu = O(\epsilon)$ . Thus the mixing matrix of the neutrinos is given by

$$U_{MNS} = U_L U_\nu^\dagger = U_L \begin{pmatrix} 1 & 0 & 0 \\ 0 & \cos \theta_\nu & -\sin \theta_\nu \\ 0 & \sin \theta_\nu & \cos \theta_\nu \end{pmatrix}, \quad (9)$$

where  $U_L$  is the unitary rotation of the left-handed charged leptons required to diagonalize  $M_L$ . Consequently,

$$\begin{aligned} \sin \theta_{atm} &= \cos \theta_\nu \sin \theta_{atm}^L - \sin \theta_\nu \cos \theta_{sol}^L \cos \theta_{atm}^L, \\ &= \sin \theta_{atm}^L - O(\epsilon) \\ \sin \theta_{13} &= \cos \theta_\nu \sin \theta_{13}^L - \sin \theta_\nu \sin \theta_{sol}^L, \\ \sin \theta_{sol} &= \sin \theta_{sol}^L, \end{aligned} \quad (10)$$

where  $\sin \theta_{atm}^L$ ,  $\sin \theta_{sol}^L$ , and  $\sin \theta_{13}^L$  are the 23, 12, and 13 elements of  $U_L$  respectively. In performing the fit to the data, we take as the neutrino mixings predicted by the model  $\sin \theta_{sol}^L$ ,  $\sin \theta_{atm}^L$ , and  $\sin \theta_{13}^L$ , i.e. the angles obtained from diagonalizing the charged lepton mass matrix. These are what are given under ‘‘model’’ for these quantities in Table III. However, we take account of the unknown  $\theta_\nu$  by including in the ‘‘experimental error’’ for  $\sin \theta_{atm}$  in Table III a ‘‘theoretical error’’ corresponding to an angle of  $\epsilon = 0.19$  rad.

In fitting, one has to take into account that the parameters appearing in Eq. (8) are, in general, complex. Because of the freedom to redefine the phases of the quark and lepton fields, most of the phases can be ‘‘rotated away’’ from the low energy theory. We will consider two cases. If the group theoretical factors denoted  $f$  and  $f_H$  are real, then there are two physical phases in the mass matrices of Eq. (8), which one can take to be phases of the parameters  $\epsilon$

and  $\delta_H$ . We will denote these by  $\theta_\epsilon$  and  $\theta_H$ . If  $f$  and  $f_H$  are complex, then there are two additional phases, which we will denote  $\theta'$  and  $\theta_{f_H}$ . The phase  $\theta'$  comes into the subleading terms of the 23 and 32 elements of  $M_D$  and  $M_L$ . The phase  $\theta_{f_H}$  comes only into the 22 element of  $M_L$ . The phase  $\theta'$  has only a small effect on the fit, and  $\theta_{f_H}$  has almost none.

Altogether, then, we fit using 9 real parameters ( $M_U, M_D, C_1, C_2, \epsilon, \delta, \delta_H, f, f_H$ ) and two or four phases ( $\theta_\epsilon, \theta_H$ , and if  $f$  and  $f_H$  are complex then also  $\theta'$  and  $\theta_{f_H}$ ). With these we fit sixteen quantities: the 9 masses of the quarks and leptons (excluding the neutrino masses, which depend on the unknown  $M_R$ ), the 3 CKM angles, the 1 CKM phase, and the 3 neutrino mixing angles.

	model (at $M_{PS}$ )	expt. (at $M_{PS}$ )	off (%)	expt. error* (%)
$m_e$	0.0004900	0.0004888	0.027	1.0*
$m_\mu$	0.1031	0.1032	-0.13	1.0*
$m_\tau$	1.756	1.754	0.07	1.0*
$m_u$	0	0.000571	100	600*
$m_c$	0.342	0.278	23.0	15.1
$m_t$	87.24	86.93	0.36	4.6
$m_s/m_d$	18.68	18.90	-1.14	4.23
$m_s$	0.0358	0.0254	40.8	31.5
$m_b$	1.17	1.186	-1.29	4.22
$\frac{m_e/m_\mu}{m_s/m_\mu}$	0.0886	0.0895	-0.99	
$m_b/m_\tau$	0.667	0.676	-1.35	
$V_{us}$	0.2243	0.2243	0.002	0.71
$V_{cb}$	0.0456	0.0463	-1.51	3.24
$ V_{ub} $	0.00368	0.00432	-14.8	11.6
$\delta_{13}$	0.887	0.995	-10.8	24.12
$\sin \theta_{sol}$	0.518	0.559	-7.33	7.51
$\sin \theta_{atm}$	0.891	0.707	26.1	28*
$\sin \theta_{13}$	0.014	< 0.178		
$\chi^2$	7.2			

Table III.

The results of the fit assuming  $f$  and  $f_H$  are real are given in Table III. The asterisks in the “experimental error” column are reminders that for certain entries a “theoretical error” is included, as explained above. The masses are all in GeV. The CKM phase  $\delta_{13}$  is in radians. One notes that most quantities are fit excellently. The least good fits are to  $m_c, m_s$ , and  $|V_{ub}|$ . Considering that 11 parameters are fitting 16 quantities, the  $\chi^2$  of 7.2 is quite reasonable.

The parameter values for this fit are  $\epsilon = 0.189, C_1 = 1.03, C_2 = -1.51, f = 0.566, f_H = 0.208, 16\pi^2\delta = 2.22, 16\pi^2\delta_H = 2.66, \theta_\epsilon = 1.52$  rad,  $\theta_H = 0.514$  rad. Note that all these quantities are of order one. In other words, no small dimensionless parameters are needed to fit the quark and lepton mass hierarchies in this model. The scales called  $m_U$  and  $m_D$  in Eq. (8) are given respectively by 86.9 GeV and 0.79 GeV. The large ratio of these scales is not explained by the structure of the model or by symmetry, and presumably comes from the details of the sector that breaks the weak interactions.

	model (at $M_{PS}$ )	expt. (at $M_{PS}$ )	off (%)	expt. error* (%)
$m_e$	0.0004888	0.0004888	-0.012	1.0*
$m_\mu$	0.1032	0.1032	-0.01	1.0*
$m_\tau$	1.755	1.754	0.02	1.0*
$m_u$	0	0.000571	100	600*
$m_c$	0.317	0.278	14.14	15.1
$m_t$	87.22	86.93	0.33	4.6
$m_s/m_d$	18.44	18.90	-2.39	4.23
$m_s$	0.0346	0.0254	36.17	31.5
$m_b$	1.17	1.186	-1.67	4.22
$\frac{m_e}{m_\mu} / \frac{m_d}{m_s}$	0.0874	0.0895	-2.39	
$m_b/m_\tau$	0.665	0.676	-1.7	
$V_{us}$	0.2243	0.2243	-0.018	0.71
$V_{cb}$	0.0458	0.0463	-1.13	3.24
$ V_{ub} $	0.00382	0.00432	-11.5	11.6
$\delta_{13}$	0.889	0.995	-10.6	24.12
$\sin \theta_{sol}$	0.499	0.559	-10.7	7.51
$\sin \theta_{atm}$	0.895	0.707	26.7	28*
$\sin \theta_{13}$	0.015	< 0.178		
$\chi^2$	6.0			

Table IV.

The results of the fit assuming  $f$  and  $f_H$  are complex are given in Table IV. The parameter values for the fit in Table IV are  $\epsilon = 0.182$ ,  $C_1 = 0.997$ ,  $C_2 = -1.60$ ,  $f = 0.573$ ,  $f_H = 0.224$ ,  $16\pi^2\delta = 2.16$ ,  $16\pi^2\delta_H = 3.22$ ,  $\theta_\epsilon = -0.554$  rad,  $\theta_H = -1.56$  rad.

Comparison of Tables III and IV shows that the inclusion of the phases  $\theta'$  and  $\theta_{fH}$  makes very little difference to the fits. This is not surprising, since  $\theta'$  appears only on subleading terms in the mass matrices, and  $\theta_{fH}$  appears on the very small entry  $f_H$ . For the two fits, the values of the real parameters hardly changes. The phase angles  $\theta_\epsilon$  and  $\theta_H$  both change by  $-2.07$  rad, but that is essentially due to a rephasing: a shift in these two phases by a certain amount can be compensated by a shift in  $\theta'$  together with a change in the phase of two small subleading terms. In other words, what is really changing a lot between the fits in Tables III and IV is the phase  $\theta'$  (which is, of course, zero for the fit in Table III). What this shows is that the fit is hardly affected by large changes in  $\theta'$ .

In this model there is a relation between the atmospheric angle and  $\theta_{13}$ , which is given in Eq. (10). Using the best-fit values given in Table III, Eq. (10) yields

$$\begin{aligned} |\sin \theta_{atm}| &= |\cos \theta_\nu(0.891) - \sin \theta_\nu(0.396)|, \\ |\sin \theta_{13}| &= |\cos \theta_\nu(-0.014) + \sin \theta_\nu(0.518)|. \end{aligned} \quad (11)$$

If the parameter  $\sin \theta_\nu$  were a real number, these equations would give a prediction for  $\theta_{13}$  in terms of  $\theta_{atm}$ . For values of the atmospheric angle near maximal mixing, i.e.  $\theta_{atm} \cong \pi/4$ , the prediction for the 13 angle would be approximately given by

$$|\sin \theta_{13}| \cong 0.160 - 0.72(\sin \theta_{atm} - 1/\sqrt{2}). \quad (12)$$

However, in fact, the parameter  $\sin \theta_\nu$  can be complex. Therefore, the smaller of the two values that is obtained for  $|\sin \theta_{13}|$  by solving Eq. (11) with real  $\sin \theta_\nu$  is a *lower bound*. So, if the atmospheric mixing angle is near maximum, there is a lower bound on  $\sin \theta_{13}$  given by Eq. (12).

## VI. CONCLUSIONS

The model that we have studied here is the first predictive grand unified model with a radiative fermion mass hierarchy. In a number of ways, it is as economical as a model of quark and lepton masses can be. The masses and

mixings of the second and third families come from only three effective Yukawa operators, shown in Eq. (1). These operators account for many features of the light fermion spectrum: (1) the fact that  $V_{cb}$  is of the same order as  $m_s/m_b$  and  $m_\mu/m_\tau$ ; (2) the fact that  $m_c/m_t$  is much smaller than those ratios; (3) the largeness of the atmospheric and solar neutrino angles; (4) the smallness of the 13 angle; (5) the rough equality of  $m_b^0$  and  $m_\tau^0$ ; and (6) the Georgi-Jarlskog factor of about 1/3 between  $m_s/m_b$  and  $m_\mu/m_\tau$ . The masses and mixings of the first family (except for the solar neutrino angle) come from loop diagrams. It is remarkable that one of these loop diagrams (Fig. 1) is present automatically, whereas the other (Fig. 2) requires only a single additional Yukawa term to be postulated.

It is striking that no small parameters are needed in this model to account for the dramatic hierarchies in the quark and lepton masses. The model yields a definite relation between the atmospheric angle and the angle  $\theta_{13}$ .

- 
- [1] H. Georgi and S.L. Glashow, *Phys. Rev.* **D7**, 2457 (1973); R.N. Mohapatra, *Phys. Rev.* **D9**, 3461 (1974); H. Georgi, “Fermion Masses in Unified Models”, in *First Workshop on Grand Unification*, ed. P.H. Frampton, S.L. Glashow, and A. Yildiz (1980), Math Sci Press, Brookline, MA).
- [2] S.M. Barr, *Phys. Rev.* **D21**, 1424 (1980); R. Barbieri and D.V. Nanopoulos, *Phys. Lett.* **B95**, 43 (1980); S.M. Barr, *Phys. Rev.* **D24**, 1895 (1981).
- [3] S.M. Barr, *Phys. Rev.* **D76**, 105024 (2007).
- [4] K.S. Babu and S.M. Barr, *Phys. Lett.* **B525**, 289 (2002).
- [5] A. Giveon, L.J. Hall, and U. Sarid, *Phys. Lett.* **B 271**, 138 (1991); S. Kelley, J.L. Lopez, and D.V. Nanopoulos, *Phys. Lett.* **B274**, 387 (1992); A. Arason, D.J. Castaño, E.J. Piard, and P. Ramond, *Phys. Rev.* **D47**, 232 (1993); V. Barger, M.S. Berger, and P. Ohmann, *Phys. Rev.* **D47**, 1093 (1993); M. Carena, S. Pokorski, and C.E.M. Wagner, *Nucl. Phys.* **B406**, 59 (1993); V. Barger, M.S. Berger, P. Ohmann, and R.J.N. Phillips, *Phys. Lett.* **B314**, 351 (1993); P. Langacker and N. Polonsky, *Phys. Rev.* **D49**, 1454 (1994).
- [6] A. Arason, D.J. Castaño, B. Kesthelyi, S. Mikaelian, E.J. Piard, P. Ramond, and B.D. Wright, *Phys. Rev.* **D46**, 3945 (1992), and refs. therein.
- [7] H. Georgi and C. Jarlskog, *Phys. Lett.* **B86**, 297 (1979).
- [8] A. V. Manohar and C. T. Sachrajda (Particle Data Group), *J. Phys.* **G33**, 1 (2006); A. Ali Khan et. al., *Phys. Rev.* **D67**, 059901 (2003); M. Della Morte et. al., *Nucl. Phys.* **B729**, 117 (2005).
- [9] G. Anderson, S. Raby, S. Dimopoulos, L.J. Hall, and G.D. Starkman, *Phys. Rev.* **D49**, 3660 (1994).
- [10] K.S. Babu and S.M. Barr, *Phys. Lett.* **B381**, 202 (1996); C.H. Albright and S.M. Barr, *Phys. Rev.* **D58**, 013002 (1998); C.H. Albright, K.S. Babu, and S.M. Barr, *Phys.Rev.Lett.* **81**, 1167 (1998); J. Sato and T. Yanagida, *Phys. Lett.* **B430**, 127 (1998); N. Irges, S. Lavignac, and P. Ramond, *Phys. Rev.* **D58**, 035003 (1998); T. Asaka, *Phys.Lett.* **B562**, 291 (2003); X.-D. Ji, Y.-C. Li, R.N. Mohapatra, *Phys.Lett.* **B633**, 755 (2006).
- [11] K.S. Babu and S.M. Barr, *Phys. Lett.* **B381**, 202 (1996); N. Haba and H. Murayama, *Phys.Rev.* **D63**, 053010 (2001); K.S. Babu and S.M. Barr, *Phys.Lett.* **B525**, 289 (2002); S.M. Barr, “Four Puzzles of Neutrino Mixing”, Talk given at 3rd Workshop on Neutrino Oscillations and Their Origin (NOON 2001), Kashiwa, Japan, 5-8 Dec 2001, Published in *Kashiwa 2001, Neutrino oscillations and their origin* p. 358, [hep-ph/0206085].
- [12] J.C. Pati and A. Salam, *Phys. Rev.* **D8**, 1240 (1973); *Phys. Rev.* **D10**, 275 (1974).
- [13] S. Dimopoulos and F. Wilczek, Report No. NSF-ITP-82-07 (unpublished); R.N. Cahn, I. Hinchliffe, and L.J. Hall, *Phys. Lett.* **B109**, 426 (1982); K.S. Babu and S.M. Barr, *Phys. Rev.* **D48**, 5354 (1993).
- [14] S. Raby (Particle Data Group), *J. Phys.* **G33**, 1 (2006).
- [15] V. Agrawal, S.M. Barr, J.F. Donoghue, and D. Seckel, *Phys. Rev.* **D57**, 5480 (1998); S.M. Barr and A. Khan, *Phys. Rev.* **D76**, 045002 (2007).
- [16] V.D. Barger, M.S. Berger, and P. Ohman, *Phys.Rev.* **D47**, 3 (1998).
- [17] Zhi-zhong Xing, He Zhang and Shun Zhou, *Phys. Rev.* **D77**, 113016 (2008); Ilja Dorner, Pavel Fileviez Prez, Germn Rodrigo, *Phys. Rev.* **D75**, 125007 (2008).
- [18] S. Eidelman et al. (Particle Data Group), *Phys. Lett.* **B592**, 1 (2004).
- [19] B. Kayser, Particle Data Group, *J. Phys.* **G33**, 1 (2006).